

**P3.1 YEARLONG EVALUATION OF URBAN HEAT ISLAND COUNTERMEASURES FROM THE VIEWPOINTS OF THERMAL ENVIRONMENT MITIGATION AND URBAN ENERGY CONSERVATION**

Yukihiro Kikegawa<sup>a,\*</sup>, Yutaka Genchi<sup>b</sup>, Hiroaki Kondo<sup>b</sup>, and Yukitaka Ohashi<sup>c</sup>  
<sup>a</sup>Global Environment Laboratory, Fuji Research Institute Corporation, Tokyo, Japan  
<sup>b</sup>National Institute of Advanced Industrial Science and Technology, Ibaraki, Japan  
<sup>c</sup>Okayama University of Science, Okayama, Japan

**1. INTRODUCTION**

In large Asian tropical or subtropical cities where anthropogenic energy demand is concentrated, urban heat island effects cause the increases in building energy demands for cooling. The recent increase rate of summer electric power demand is estimated up to 3%/°C in the Greater Tokyo, this means the fact that about 1.6GW of additional demand is required as the regional air temperature increases by 1.0 °C. This huge demand for summer electricity creates additional waste heat, which would further intensify Tokyo urban heat island. From the viewpoint of the reduction of anthropogenic CO<sub>2</sub> emission to mitigate the global warming, this additional energy demand should be reduced through the control of the urban heat islands.

In order to analyze the above-mentioned vicious interaction between urban thermal environment and cooling energy use on city-scale, and to evaluate the technologies and measures for urban warming alleviation, we have been developed a new multi-scale numerical simulation system.

In this study, our system was improved and validated for the yearlong numerical prediction of the regional air-conditioning energy consumption in several types of urban districts. Then, the improved system was applied to Tokyo urban canopies to assess the yearlong impacts of heat island countermeasures on urban thermal environment and building energy consumption.

**2. THE MODELS**

The developed simulation system consists of three numerical models as shown in Figure1. Those are MM, CM, and BEM. MM is a three-dimensional mesoscale meteorological model which adopt the Boussinesq approximated equations with the hydrostatic assumption (Kondo, 1995). Its operational horizontal grid size is about 10km × 10km. In vertical direction, the terrain-following coordinate system is used dividing the atmosphere into 40 levels from the ground up to 6200m high. The closure model of Gambo (1978) is adopted to determine the vertical diffusivities in the upper boundary layer. In the surface boundary layer, Monin-Obukhov similarity theory is used to calculate the surface fluxes of heat and momentum over rural area. As for the urban area, CM is introduced to take account of the urban canopy effect on the boundary layer.

CM is a one-dimensional urban canopy model (Kondo and Liu, 1998). In CM, the geometrical structure of an urban block in 0.5 to 1km square is

simply parameterized with the mean width of the buildings, mean width of the roads and distribution of the height of the buildings (Fig.1). These parameters are derived based on high-resolution GIS polygon data. In the urban block model, heat fluxes from the roof, wall and road are separately computed through heat balance equation on each surface in the canopy. Anthropogenic heat sources are also considered at each level. Additionally, the effect of complicated radiation processes among the buildings were considered to some extent, such as shading effect and reflection of short wave, and re-emission of long wave from building and ground surfaces.

For the consideration of the dynamical variations of the anthropogenic heat released from air-conditioning systems, BEM was developed (Kondo and Kikegawa, 2003). BEM is a simple sub model for building energy analysis, and the anthropogenic heat from buildings was calculated based on the air temperature and humidity in the urban canopy. BEM is a box-type heat budget model where a building in the urban block is treated as a box, and the cooling load in the buildings are calculated for the sensible and the latent heat components, separately (Fig.1).

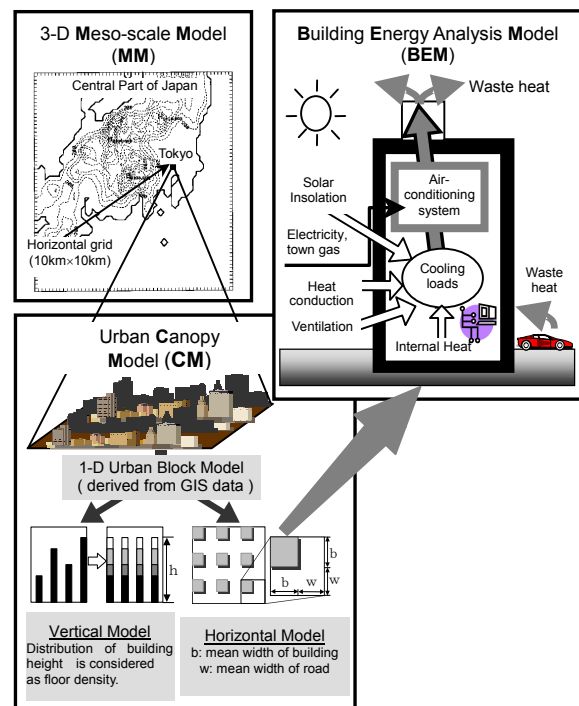


Fig.1 Composition of Simulation System

Thus, BEM can express the responses of air-conditioning energy consumption and its consequent waste heat emission to canopy meteorological conditions predicted by CM. The CM

\* Corresponding author address: Yukihiro Kikegawa, Fuji Research Institute Corp., Global Environment Laboratory, 2-3 Kandanshiki-cho, Chiyoda-ku, Tokyo 101-8443 Japan; e-mail: [kike@cyq.fuji-ric.co.jp](mailto:kike@cyq.fuji-ric.co.jp)

was improved so it could express the feedback process of buildings' anthropogenic heat to canopy atmospheric heat balance, and CM was combined with BEM (Fig.2). In addition, the CM-BEM combined model and MM were also coupled via a bi-directional scheme. The CM-BEM computational results for heat and momentum vertical fluxes in the surface boundary layer were adopted as bottom boundary flux conditions for the upper MM atmosphere (Fig.3).

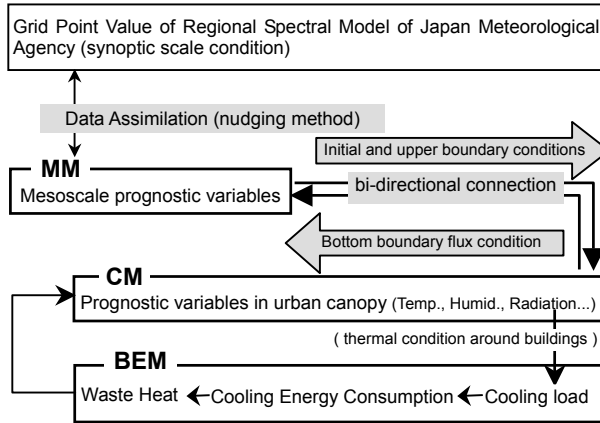
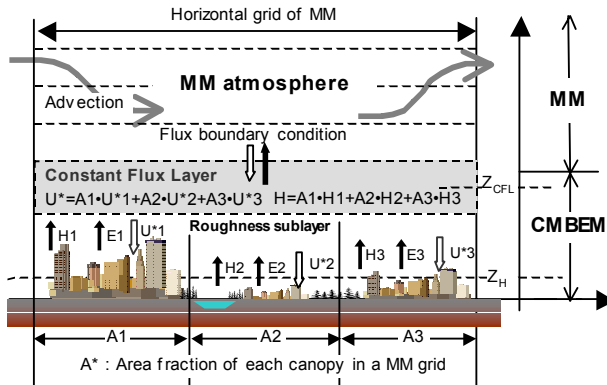


Fig.2 Computational Flow on MM-CM-BEM



$U^*$  : Momentum flux,  $H$  : Sensible heat flux,  $E$  : Latent heat flux,  $Z_H$  : Averaged building height  
 $Z_{CFL}$  : Height of constant flux layer  $\approx 1.5Z_H \sim 3.0Z_H$  [after Roth(2000), Wieringa (1993)]

Fig.3 Connection Scheme between MM & CM-BEM

### 3. MODEL IMPROVEMENT

In our past studies, we applied the above-mentioned simulation system (MM-CM-BEM) to Tokyo metropolitan area under summer conditions, and confirmed its validity in numerical prediction of urban canopy meteorological elements and regional energy demands for cooling (Kikegawa, et al., 2003; Kondo and Kikegawa, 2003). However, in most of Japanese cities under temperate monsoon climate including Tokyo, we need air-conditioning not only for cooling but also for heating mainly in winter, when measures for urban heat-island alleviation could produce negative effects on energy conservation in contrast with positive effects in summer. So, toward

comprehensive assessment of urban heat island countermeasures including their impacts on urban energy consumption and its consequent CO<sub>2</sub> emission, year-round evaluation of measures should be conducted.

For the above-mentioned reason, we introduced several improvements in our system to expand its applicability to yearlong prediction of urban thermal environment and its corresponding change in air-conditioning energy use. Because meteorological calculation components of our system, MM and CM, were the models with applicability to any seasonal conditions, only BEM was improved for yearlong calculation as follows.

Heating system of building was additionally modeled in BEM. Adopting electric air-source heat-pump and town-gas-driven heating equipment as typical heating system, the calculation part for anthropogenic heat was improved using following equation.

$$Q_{AS} = (H_{out} + E_{out}) - E_C = \frac{COP - 1}{COP} (H_{out} + E_{out}) \quad (1)$$

Eq.(1) represents heat balance of air-conditioning system which adopts an air-source heat-pump.  $Q_{AS}$  stands for the sensible heat taken from outdoor air by heat pump.  $E_C$  and COP indicate the electric power consumption and the coefficient of performance of heat pump, respectively. Here, COP corresponds to the energy efficiency ratio of the system. Remaining  $H_{out}$  and  $E_{out}$  indicate the sensible and the latent heat supplied from the system for room heating. Eq.(1) was used to calculate the air-conditioning waste heat from heat pumps in heating operation, which corresponds to  $Q_{AS}$  and becomes negative value meaning heat absorption from the atmosphere in winter. In cooling operation, eq.(2) was used instead of eq.(1) to calculate positive value of  $Q_{AS}$ , i.e. anthropogenic heat release from heat pump system to the atmosphere.

$$Q_{AS} = E_C + (H_{out} + E_{out}) = \frac{COP + 1}{COP} (H_{out} + E_{out}) \quad (2)$$

As for the air-conditioning system that adopts town-gas-driven heating equipments, such as boilers, eq.(3) was used to calculate waste heat.

$$Q_A = \frac{1 - \eta}{\eta} (H_{out} + E_{out}) \quad (3)$$

Here,  $Q_A$  denotes the total waste heat. And  $\eta$  represents the thermal efficiency ratio of heating equipment.  $Q_A$  was separated into the sensible and the latent heat component based on the ratio of the higher calorific value to the lower calorific value of town gas, and was considered as anthropogenic heat source in sensible and latent heat balance of the urban canopy atmosphere in CM.

Except for the abovementioned improvements concerning the calculation of waste heat from heating systems, the same BEM simulation scheme that is used under summer conditions is adopted for the year-round simulation to predict architectural heat balance in the urban canopy. This was reasonable, because the remaining equations in BEM were unchangingly applicable to any seasonal conditions.

## 4. MODEL VERIFICATION

### 4.1 Validation of BEM in housing condition

The performance of the improved BEM was examined through yearlong comparative simulation, using another building energy program named SMASH. SMASH stands for simplified analysis system for housing air conditioning energy, and is the most standard practical-use model in Japan for housing energy simulation. Both SMASH and BEM are box-type building heat budget models for unsteady state air conditioning energy simulation. Taking account of this common feature and the proven reliability of SMASH, we selected SMASH as a standard model in the comparative simulation.

Then yearlong simulations of BEM and SMASH were carried out adopting a same apartment building prototype, that was a five-storied reinforced concrete construction building composed of ten apartments each of which has the same floor area of 81 m<sup>2</sup>. As for parameters with relation to air-conditioning energy simulation such as thermal properties of building materials and temporal schedule of air-conditioning and indoor heat generation, default setups in SMASH were equally adopted for BEM. In addition, the standard climate data of Tokyo was input both to BEM and SMASH as the ambient weather conditions.

Computational results of the yearlong simulation were then compared between BEM and SMASH. As a result, it was confirmed that BEM was roughly able to reproduce the temporal variation of the spatially averaged room temperature calculated by SMASH (Fig.4). With respect to daily averaged room temperatures, a fair linear correlation was recognized between BEM and SMASH (Fig.5).

Fig.6 & Fig.7 show comparisons of simulated cooling and heating loads between BEM and SMASH. The temporal patterns of hourly load variations were nearly in good agreement between the two models (Fig.6). The daily total loads indicated a clear linear correlation over the yearlong simulation period (Fig.7), but BEM tended to slightly overestimate the loads mainly in cooling conditions compared to SMASH (Fig.7). The root mean square error, i.e. the standard deviation of error, was estimated to be about 100Wh/day/floor-m<sup>2</sup> over the entire simulation period. This discrepancy in the air-conditioning load calculation was considered to be caused by the difference in physical models between SMASH and BEM, that is to say SMASH is sophisticated multi-room heat budget model, whereas BEM is more simple single-room model.

Based on the abovementioned results, and taking account of the difference in complexity between BEM and SMASH, we concluded that the improved BEM was almost adequately able to reproduce the yearlong temporal variations of housing thermal conditions with relation to air-conditioning energy consumption in spite of its simplicity.

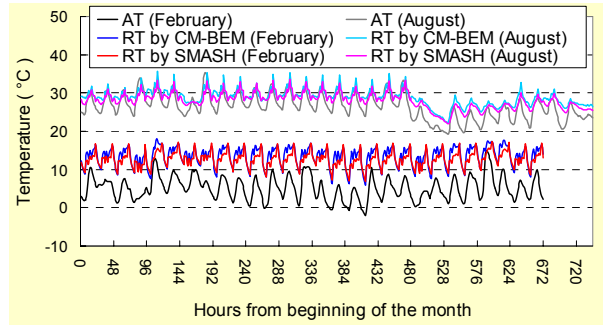


Fig.4 Temporal variations of room temperatures calculated by CM-BEM & SMASH for an apartment building prototype. RT and AT stand for room temperature and ambient air temperature.

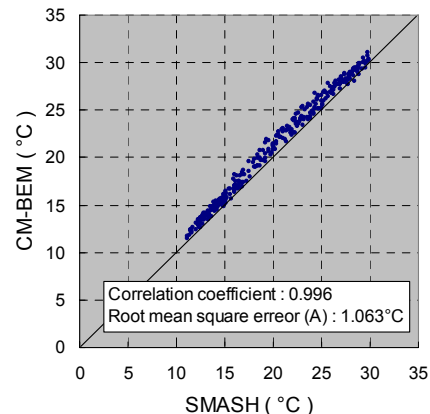


Fig.5 Yearlong comparison of daily-averaged simulated room temperatures between CM-BEM & SMASH.

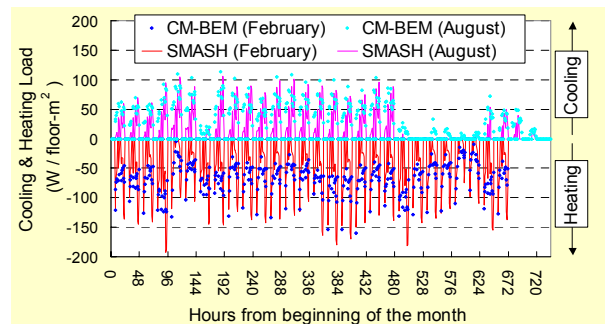


Fig.6 Temporal variations of cooling and heating loads simulated by CM-BEM & SMASH for an apartment building prototype. Depicted load corresponds to sensible heat component of thermal load per unit floor area.

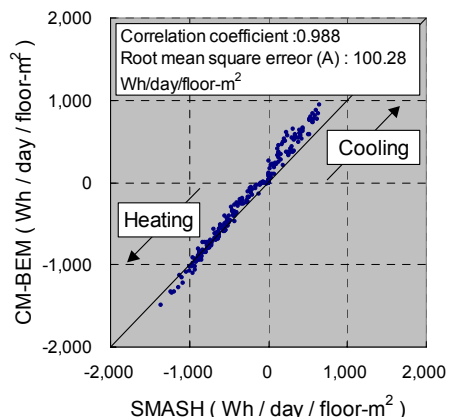


Fig.7 Yearlong comparison of daily-total sensible heat component of cooling and heating load.

## 4.2 Validation of CM-BEM in business district (Reproducibility of temperature sensitivity of regional electricity demand)

Next, the improved BEM was applied to the Nihonbashi area, which mainly consists of middle-rise office buildings and is located near the center of Tokyo metropolitan area (Fig.10). Adopting the initial and boundary conditions for CM atmosphere and parameters setup for BEM as described in the following chapter 5 (see Tab.2 & Tab.3), yearlong simulation was carried out using CM-BEM coupled model shown in Fig.2.

For the model validation from the aspect of the regional energy demand prediction, we obtained the actual data on the hourly electric power consumption in the Nihonbashi area during summer in 2002. Then the temperature sensitivity analysis of regional electric power demand was conducted following the method in Kikegawa et al. (2003). Fig.8 shows an example of the analysis, in which the temperature sensitivity of regional electric power demand for cooling was estimated to be 10.1% / °C on average at 1500LST on weekdays. This result means that the cooling electric power demand increases by 10.1% with 1°C air temperature rise at 1500LST in the Nihonbashi area.

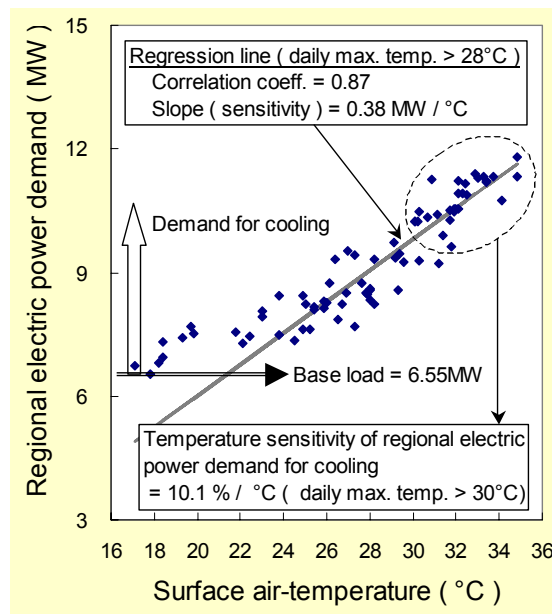


Fig.8 An example of temperature sensitivity analysis of cooling electric power demand in Nihonbashi area at 1500LST during weekdays from June to September 2002.

Following the method shown in Fig.8, hourly actual sensitivity was evaluated for daytime period (from 9 to 17h.), which corresponds to the typical working hours when most of the air-conditioning systems in the office buildings are operated in the Nihonbashi area. Then, actual sensitivities were compared with those simulated by CM-BEM, which was run twice in the yearlong simulation. In the first run, thermally insulated walls and roofs were set to the buildings, whereas the buildings were assumed to be non-insulated in the second run. Then, sensitivities were calculated based on the relation between spatially averaged air temperature computed by CM and cooling electric power consumptions in the buildings predicted by

BEM using the same method as applied to actual data as shown in Fig.8.

Lastly, the actual and simulated sensitivities were compared in Fig.9. It was confirmed that the actual sensitivities stayed in the range of simulated sensitivities between the insulated case and the non-insulated case. Unfortunately, it was impossible to set the parameters for thermal insulation consistent with the real conditions of the buildings in the Nihonbashi area because of the complexity and the diversity of buildings structure there. However, taking it into account that the temperature sensitivity of building cooling energy demand could be dominantly influenced by the degree of thermal insulation, and that the actual states of insulation of the buildings exist between the two simulated cases, it was concluded that CM-BEM was reasonably able to reproduce the interaction between the regional air-conditioning energy demand and the urban canopy air temperature.

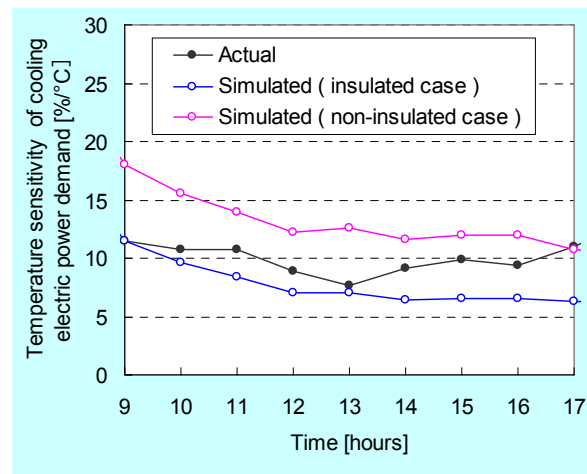


Fig.9 Temporal variations of actual and simulated temperature sensitivity of cooling electric power demand in Nihonbashi area under tropical days condition in 2002.

## 5. EVALUATION OF COUNTERMEASURES

### 5.1 Simulation conditions

Finally, the validated CM-BEM coupled model was applied to yearlong simulations to estimate the urban-block scale impacts of the heat island countermeasures. In addition to the Nihonbashi area, the Sugunami area was chosen as the computational domain from Tokyo metropolitan area (Fig.10). The Sugunami area is a typical residential district which consists of low-rise houses, and has the contrastive structure to the Nihonbashi office buildings area. The geometrical parameters of the canopies were set based on the analysis of Tokyo Geographic Information System (GIS) data over the both areas as shown in Tab.1.

Tab.1 Geometrical parameters of canopies

	Averaged Building-Width (m)	Averaged Street-Width (m)	Averaged Building-Height (m)	Averaged Sky-View-Factor (-)
Nihonbashi area (business district)	14.41	6.28	25.33	0.20
Suginami area (residential district)	10.12	6.91	6.87	0.60

As for the Initial and boundary conditions of CM, set up is done as shown in Tab.2. And the parameters set up in BEM are shown in Tab.3. Other parameters, which are not displayed in Tab.3, such as thermal properties of building materials and temporal schedule of occupancy, etc., are referred from Kikegawa et al. (2003) including the set up of exhaust heat emitted from automobiles.

Tab.4 displays the calculation cases set up in the yearlong simulations. As the measures for the urban warming alleviation, the albedo-increase and the greening of the building surfaces are adopted in addition to the reduction of the air-conditioning waste heat emission.

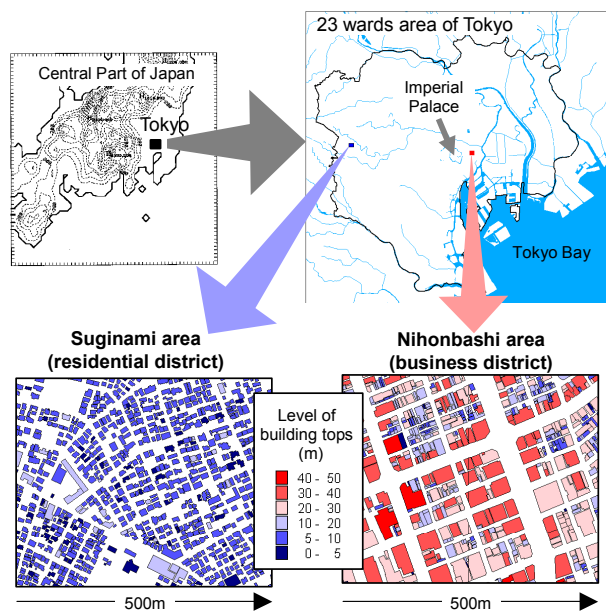


Fig.10 Computational domain (Suginami & Nihonbashi area)

Tab.2 Initial and boundary conditions used in CM-BEM simulation

Model integration period	From 0000JST 1 June 2002 to 0000JST 1 June 2003
Initial potential temperature	Linear vertical profile obtained from the upper meteorological data ( lapse rate : 1.54K/km , surface : 20°C)
Initial humidity	Constant relative humidity ( = 80% ) for all the layer
Temperature & humidity variations at upper boundary	Temporal variation rates estimated from surface observations at Tokyo district meteorological observatory
Wind variations at upper boundary	Upper wind estimated from surface observations based on logarithmic law
Short-wave downward radiation fluxes	Hourly observed values
Long-wave downward radiation fluxes	Estimated values; typical seasonal variations approximated by cosine-curve
Initial wall & roof temperature	22.3°C
Initial soil temperature	26°C
Grid structure (Atmospheric layer)	Height of the model top: 350m Grid interval: 3m-20m

Tab.4 Simulation cases set up

Case	Conditions
CASE-0	Control run No countermeasures
CASE-1	Cut-off of air-conditioning waste heat Waste heat is released not into the atmosphere but elsewhere such as sewage or soil.
CASE-2	Rooftop greening •Vegetation coverage : 50% •Surface conductance : 3mm/sec
CASE-3	Sidewall greening •Vegetation coverage : 50% (except for window) •Surface conductance : 3mm/sec
CASE-4	Rooftop albedo increase •Target : 100% area of rooftop •albedo : 0.8
CASE-5	Sidewall albedo increase •Target : 100% area of wall except for window •albedo : 0.8

Tab.3 Parameters set up in BEM calculation

		Nihonbashi area (business district)	Suginami area (residential district)
Air-conditioning	Constitution of heat source (Aggregated ratio)	Cooling •Gas-fired absorption hot and chilled water generator with cooling tower : 33% •Air-source heat pump : 67% Heating •Air-source heat pump : 50% •Boiler : 50%	Cooling •Air-source heat pump : 100% Heating •Air-source heat pump : 50% •Stove & fan heater : 50%
	Period of operation	Cooling : May.1 - Oct.31 Heating : Jan.1 - Feb.28, Dec.1 - Dec.31	Cooling : Jun.22 - Sep.29 Heating : Jan.1 - Apr.22, Nov.2 - Dec.31
	Target temp. & humidity	Cooling : Temp. = 26°C , Humid. = 50% Heating : Temp. = 22°C ( no humidity control )	Cooling : Temp. = 27°C, Humid. = 60% Heating : Temp. = 18°C ( no humidity control )
	Position of waste heat emission	Rooftop of building	Each story of house
Others	Land & surface cover	Wall : window coverage = 30% Ground : concrete = 100%	Wall : window coverage = 18% Ground : vegetation = 12.7% concrete = 87.3%
	Property	Albedo : concrete 0.2, window 0.4	Emissivity : window 0.87, others 0.97

## 5.2 Computational results

Fig.11 displays the monthly averaged differences in the simulated surface air temperatures between cases in the Nihonbashi & Sugunami area. Temperature differences were calculated, taking results in CASE-0 (no-countermeasure-case) as standards.

In summer, the maximum temperature decrease up to 0.4°C was predicted in CASE-1, i.e. in the reduction case of air-conditioning waste heat, for the Nihonbashi area. In the other seasons, the increase in sidewall albedo (CASE-5) resulted in the maximum temperature decrease up to 0.5°C. On the contrary, winter temperature increase more than 0.1°C was simulated in CASE-1. This increase was caused by the cut-off of the heat absorption from the atmosphere in the air-source heat pump operation in winter.

On the other hand, in the Sugunami area, the measure with increase in rooftop albedo (CASE-4) resulted in the maximum temperature decrease (0.2°C – 0.5°C) among cases through the all seasons. In the Sugunami area, which mainly consists of one to two story low-rise houses, the surface area of sidewalls decrease, and the anthropogenic heat is much less than that in the Nihonbashi office buildings area. Therefore, the measure to cool the rooftop surfaces (CASE-4) worked more effectively for temperature mitigation than the measure for waste heat reduction (CASE-1). The winter temperature increase up to 0.2°C was also predicted in CASE-1 owing to the same cause as that in the Nihonbashi area.

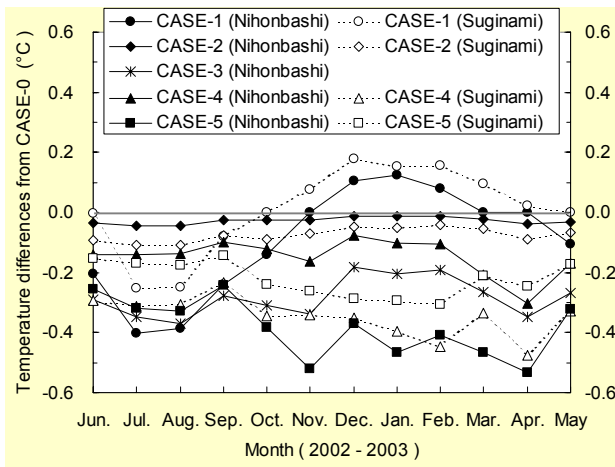


Fig.11 Monthly averaged differences in simulated surface air temperatures between cases in the Nihonbashi & Sugunami area.

In Fig.12, the regional-averaged simulated values of the monthly total energy demands for air conditioning are displayed with respect to CASE-0 as per-floor-area values. In the office buildings of the Nihonbashi area, more cooling energy demands were predicted in summer compared to heating energy demands in winter. On the contrary, the more energy demands for heating were simulated than those for cooling in the houses of the Sugunami area. These results were roughly consistent with the actual states in the buildings located in Tokyo.

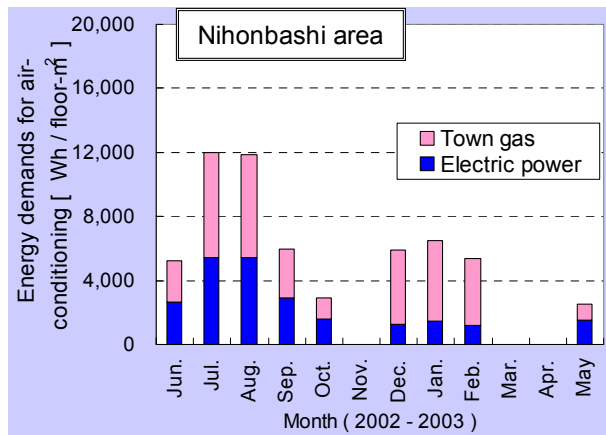
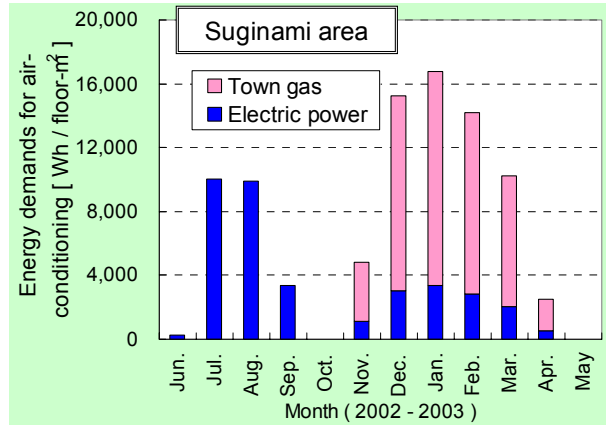


Fig.12 Regional-averaged per-floor-area values of monthly totalized energy demands for air conditioning in the Nihonbashi & Sugunami area ( CASE-0 ).

Finally, the year-round impacts of the heat island measures on the building energy consumptions were analyzed. Their results are displayed in Fig.13. Here, CASE-0 is chosen as the control-run again.

In Fig.13, differences in the monthly-totalized air-conditioning energy demands from CASE-0 are indicated in percentages. In the Nihonbashi area, the total air-conditioning energy demands were saved in the all cases of measures shown in Tab.4 owing to summer temperature decreases and their consequent cooling energy savings. Although the increases in heating energy demands were predicted in the albedo-increase and the greening cases because of temperature decrease in winter, these negative effects were entirely compensated by the cooling energy savings in summer.

On the contrary, the totals of the simulated air-conditioning energy demands were not saved and increased in the high-albedo and greening cases in the Sugunami area. Those negative effects were caused by the dominant increases in the heating energy demands resulted from temperature decreases in winter, which could not be compensated by the less decreases in the cooling energy demands in summer. From the viewpoint of the energy conservation, the reduction of air-conditioning waste heat (CASE-1) was the best measure which produced the year-round saving effect on the air-conditioning energy in the Sugunami area. This positive result was attributed to the temperature decrease in summer and the increases in winter. (Fig.11).

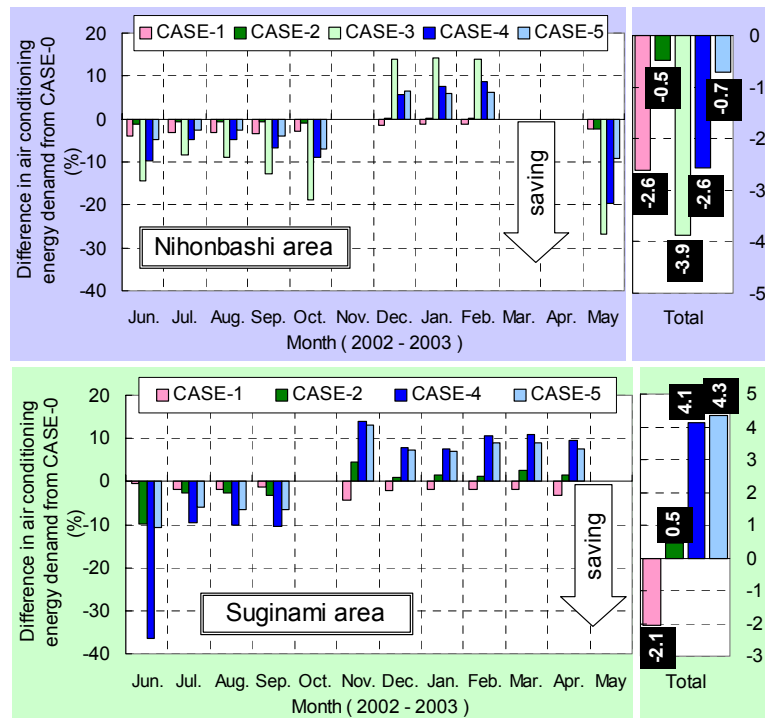


Fig.13 Differences in monthly totalized air-conditioning energy demands between cases in Nihonbashi & Suginami area.

## 6. CONCLUSIONS

In this study, the Building Energy Analysis Model (BEM) was improved and validated for the yearlong numerical prediction of the air-conditioning energy consumption in the buildings. We combined the improved BEM with the Urban Canopy Model (CM) towards the yearlong evaluation of urban warming countermeasures. The combined model, CM-BEM, was then applied to the two contrastive urban districts in Tokyo. One was Nihonbashi area, and the other Suginami area. The former consists of middle-rise office buildings, and the latter of low houses. The following results were obtained from numerical experiments, which were conducted to simulate the yearlong interaction between the near-ground meteorological conditions and the buildings' air-conditioning energy consumptions in the urban canopies.

- 1) The performance of the improved BEM was examined through yearlong comparative simulation of housing energy demands for the air-conditioning. SMASH, a practical and state-of-the-art simulation code, was used as a standard model. As results, it was confirmed that BEM was roughly able to reproduce the yearlong temporal variations of housing thermal conditions such as room temperatures and cooling & heating loads.
- 2) In Nihonbashi area, the simulated sensitivities of cooling electric power demands to the air temperature were roughly consistent with actual regional sensitivities, which were estimated by using the actual electricity demand data in the area.

Based on the results described in 1) and 2), the applicability of CM-BEM to yearlong simulation was verified.

- 3) Finally, the annual impacts of several heat-island countermeasures were evaluated from the both viewpoints of the air temperature alleviation and the cooling and heating energy conservation. As results, several effective measures to mitigate summertime air temperature, such as albedo increase and greening of buildings' surfaces, were predicted to result in annual increases in the air-conditioning energy demands in some cases. Those negative effects were attributed to the wintertime temperature decrease and its consequential increase in heating energy. The importance to assess the yearlong impacts of countermeasures on the urban thermal environment and the building energy demand was clarified.

## REFERENCES

- Gambo, K., 1978: Notes on the turbulence closure model for atmospheric boundary layers, *J. Meteor. Soc. of Japan*, 56, 466-480.
- Kikegawa, Y., Y. Genchi, H. Yoshikado, and H. Kondo, 2003: Development of a Numerical Simulation System toward Comprehensive Assessments of Urban Warming Countermeasures including Their Impacts upon the Urban Building's Energy-demands, *Applied Energy*, 76, 449-466.
- Kondo, H., 1995: The Thermally Induced Local Wind and Surface Inversion over the Kanto Plain on Calm Winter Nights, *J. Appl. Meteor.* 34(6), 1439-1448.
- Kondo, H. and Liu, F.H., 1998: A study on the urban thermal environment obtained through one-dimensional urban canopy model, *J. of Japan Soc. Atmos. Environ.*, 33, 179-192(in Japanese).
- Kondo, H. and Y. Kikegawa, 2003: Temperature Variation in the Urban Canopy with Anthropogenic Energy Use, *Pure and Applied Geophysics*, 160, 317-324.
- Roth, M., 2000: Review of atmospheric turbulence over cities, *Q. J. R. Meteorol. Soc.*, 126, 941-990.
- Wieringa, J., 1993: Representative roughness parameters for homogeneous terrain, *Boundary-Layer Met.*, 63, 323-363.